



Optimal control of a nonlinear fed-batch fermentation process using model predictive approach

Ahmad Ashoori^{a,*}, Behzad Moshiri^a, Ali Khaki-Sedigh^b, Mohammad Reza Bakhtiari^c

^aControl and Intelligent Processing Center of Excellence, School of Electrical and Computer Engineering, University of Tehran, Unit 4, No. 103, 73rd Square, Janbazan Gharbi Street, Hafthoz, Tehran, Iran

^bDepartment of Electrical Engineering, K.N. Toosi University of Technology, Tehran, Iran

^cIranian Research Organization for Science and Technology, Iran

ARTICLE INFO

Article history:

Received 7 July 2008

Received in revised form 16 March 2009

Accepted 19 March 2009

Keywords:

Fed-batch fermentation process

Penicillin production

Model predictive control

Nonlinear model

LoLiMoT

ABSTRACT

Bioprocesses are involved in producing different pharmaceutical products. Complicated dynamics, non-linearity and non-stationarity make controlling them a very delicate task. The main control goal is to get a pure product with a high concentration, which commonly is achieved by regulating temperature or pH at certain levels. This paper discusses model predictive control (MPC) based on a detailed unstructured model for penicillin production in a fed-batch fermentor. The novel approach used here is to use the inverse of penicillin concentration as a cost function instead of a common quadratic regulating one in an optimization block. The result of applying the obtained controller has been displayed and compared with the results of an auto-tuned PID controller used in previous works. Moreover, to avoid high computational cost, the nonlinear model is substituted with neuro-fuzzy piecewise linear models obtained from a method called locally linear model tree (LoLiMoT).

© 2009 Elsevier Ltd. All rights reserved.

1. Introduction

Bioprocesses, which are involved in producing different pharmaceutical products, may conveniently be classified according to the mode chosen for the process: either batch, fed-batch or continuous. From the control engineer's viewpoint, they are fed-batch processes that present the greatest challenge because the model of the plant is usually given as a black-box model, i.e. no mathematical model is available. Moreover, both the initial states of the process and the parameters of the model may vary randomly from batch to batch [1]. For the same input, the output of each batch would not be the same. Antibiotics such as penicillin are made in fed-batches commercially, and there is a great economic incentive to optimize such processes [2]. Controlling the following parameters has significant importance dealing with these processes: (a) temperature; if it falls down, the proteins' reactions slow down and if it rises the proteins will denature. (b) pH; suitable pH prepares the environment for proper transfer of feedstuff and energy/redundant stuff to and from the cell membrane respectively. (c) Dissolved oxygen (DO_2); cells cannot do their vital actions without oxygen. Control of either temperature, pH or DO_2

is necessary depending on the product type, setup configuration and environmental conditions [2,3]. A typical fermentor is depicted in Fig. 1 [4].

Bioprocesses have complicated dynamics, therefore their control is a challenging and delicate task; they also are inherently concerned with nonlinearity and non-stationarity, which make modeling and parameter estimation particularly difficult. Moreover, the scarcity of on-line measurements of the component concentrations makes this task more sophisticated [5]. Hence, conventional control methods do not succeed in such task [6–8].

Temperature and pH control of bioreactors have been an interesting problem from both implementation and controller design points of view [3]. This is particularly true if the complex microbial interactions cause significant nonlinear behaviour. When this occurs, conventional control strategies may not succeed and more advanced strategies are needed. Previous studies reported various types of model-based [9–16] and intelligent [17–26] controller designs, while these control techniques may be successful for open-loop stable processes or in the vicinity of an unstable operating point [27], about which a linearization is applied, and they are often inadequate for highly unstable nonlinear bioreactors. However, attempts to develop an advanced method for controlling bioprocesses variables still continue. This is because pure product, which is the main goal of control, would be achieved using a fine control, whose way goes through model-based control methods. Model-free methods due to lack of detailed information of the system model can not lead to a high performance controller.

* Corresponding author. Tel.: +98 912 2793516/21 77929325; fax: +98 21 8831 8816.

E-mail addresses: a.ashoori@ece.ut.ac.ir (A. Ashoori), moshiri@ut.ac.ir (B. Moshiri), sedigh@kntu.ac.ir (A. Khaki-Sedigh), bakhtiari@irost.ir (M.R. Bakhtiari).

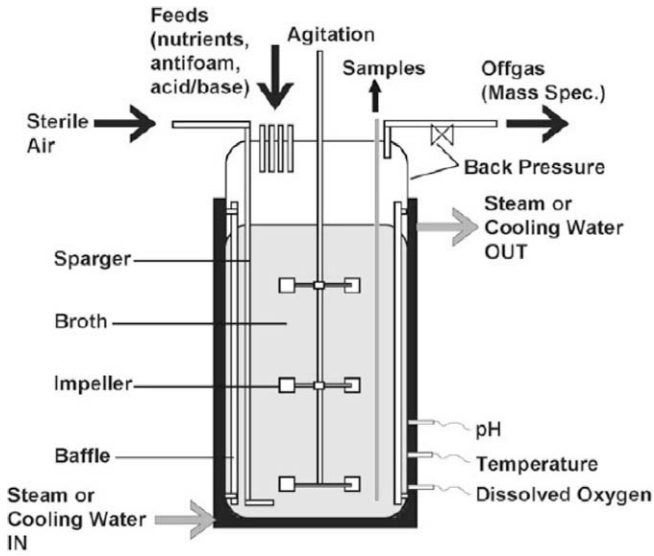


Fig. 1. A typical fermentor.

Predictive control has become a popular topic in the recent years. Model predictive control (MPC) is used in several industrial processes nowadays [9]. It has been successful in dealing with delayed systems that have constraints on the state or the control signal. This approach has proven to be feasible for online optimization and has acceptable performance as well. Its nonlinear [10] and multiple-model [11] version is also very popular in overcoming the aforementioned drawbacks.

In this article, MPC is utilized based on a detailed unstructured model for penicillin production in a fed-batch fermentor. Section 2 discusses about the model, which extends the mechanistic model of Bajpai and Reuss [28] by adding some input variables as introduced in [29]. To avoid high computational cost, obtaining the appropriate control signal using linear MPC for a linearized model of penicillin fermentation is discussed in Section 3. Section 4 discusses about performing MPC on the nonlinear model. The results of utilizing this controller to maximize penicillin concentration have been illustrated and also compared with the results of auto-tuned PID controller used in [29]. In Section 5, this method has been modified to have lower computational cost using LoLiMoT method for identifying locally linear models and exploiting them instead of the nonlinear model for prediction. Finally, the advantages and drawbacks of these methods are concluded in Section 6.

2. Model formulation

Extensive research has generated new information on the mechanisms of cellular reactions and morphological features of the mycelia and their role in the synthesis of penicillin. Given a choice of mechanisms, models of different degrees of complexity, for both cellular differentiation and bioreactor performance, have been proposed. The more complex models require and provide more information [30,31], but they are also more difficult to evaluate and apply in automatic control systems for production-scale bioreactors [32,33].

Fed-batch penicillin fermentation process data are generated using a detailed mathematical model and a simulator [29]. The model has five input variables, nine process variables, and five quality variables. Penicillin fermentation has four physiological phases (lag, exponential cell growth, stationary, and cell death) and two operational phases. The first two physiological phases are conducted as batch operation (first operational phase) while

Table 1

Functional relationship among the process variables.

Model structure
$X = f(X, S, C_L, H, T)$
$S = f(X, S, C_L, H, T)$
$C_L = f(X, S, C_L, H, T)$
$P = f(X, S, C_L, H, T, P)$
$CO_2 = f(X, H, T)$
$H = f(X, H, T)$

X , biomass concentration; S , substrate concentration; C_L , dissolved oxygen concentration; P , penicillin concentration; CO_2 , carbon dioxide concentration; H , hydrogen ion concentration for pH; T , temperature.

the last two are conducted as fed-batch operation [10]. In the first operational phase, fermentation is carried out in a batch mode to promote biomass growth resulting in high cell densities. The second operational phase is a fed-batch operation where glucose is fed until the end of the fed-batch operation. Functional relationships among the process variables are completely introduced in [29] and summarized in Table 1.

Experimental findings suggest a high degree of dependence of biomass growth on both the carbon source (glucose) and oxygen as substrates [28]. The biomass growth is also known to be inhibited by high amounts of biomass itself in penicillin fermentation. The dependence of specific growth rate on carbon and oxygen substrates was assumed to follow Contois kinetics [28] to consider the biomass inhibition. The biomass growth has been described as:

$$\frac{dX}{dt} = \mu X - \frac{X}{V} \frac{dV}{dt} \quad (1)$$

in which the specific growth rate μ as introduced in [29] is:

$$\mu = \left[\frac{\mu_x}{1 + [K_1/[H^+]] + [[H^+]/K_2]} \right] \frac{S}{(K_x X + S)} \times \frac{C_L}{(K_{ox} X + C_L)} \left[k_g e^{-\frac{E_g}{RT}} \right] - \left[k_d e^{-\frac{E_d}{RT}} \right] \quad (2)$$

in order to take into account the environmental parameters such as pH and temperature. The variables and parameters used are defined in Table 2 [29].

Since the pH of the culture medium has a tendency towards acidity, as the concentration of biomass increases, the amount of NH_4OH added into the culture medium also increases. Based on this observation, the hydrogen ion concentration $[H^+]$ is related to biomass formation as:

$$\frac{dH^+}{dt} = \gamma \left(\mu X - \frac{FX}{V} \right) + \left[\frac{-B + \sqrt{(B^2 + 4 \times 10^{-14})}}{2} - [H^+] \right] \frac{1}{\Delta t} \quad (3)$$

where B is:

$$B = \frac{|10^{-14}/[H^+] - [H^+]|V - C_{a/b}(F_a + F_b)\Delta t}{V + (F_a + F_b)\Delta t} \quad (4)$$

F_a and F_b represent acid and base flow rates in l/h, respectively, where, the concentrations in both solutions are typically assumed equal as $C_{a/b} = 3 \text{ Mol/L}$ [29].

Moreover, the influence of temperature on the specific growth rate of a microorganism shows an increasing tendency with an increase in temperature up to a certain value, which is microorganism specific and a rapid decrease is observed beyond this value. This decrease might be treated as a death rate [34]. Here, the effect of temperature on the specific growth rate has been introduced as an Arrhenius type of kinetics in Eq. (2).

The production of penicillin is described by non-growth associated product formation kinetics. The hydrolysis of penicillin is also included in the rate expression [28]:

Table 2
Initial conditions, kinetic and controller parameters for nominal operation 29.

Time t (h)	Value
<i>Initial conditions</i>	
Substrate concentration: S (g/l)	15
Dissolved oxygen concentration: $C_L (= C_L^*$ at saturation) (g/l)	1.16
Biomass concentration: X (g/l)	0.1
Penicillin concentration: P (g/l)	0
Culture volume: V (l)	100
Carbon dioxide concentration: CO_2 (mmol/l)	0.5
Hydrogen ion concentration: $[H^+]$ (mol/l)	$10^{-5.1}$
Temperature: T (k)	297
Heat generation: Q_{rxn} (cal)	0
<i>Kinetic and parameters and variables</i>	
Feed substrate concentration: s_f (g/l)	600
Feed flow rate of substrate: F (l/h)	
Feed temperature of substrate: T_f (K)	298
Yield constant: $Y_{x/s}$ (g biomass/g glucose)	0.45
Yield constant: $Y_{x/o}$ (g biomass/g oxygen)	0.04
Yield constant: $Y_{p/s}$ (g penicillin/g glucose)	0.90
Yield constant: $Y_{p/o}$ (g penicillin/g oxygen)	0.20
Constant: K_1 (mol/l)	10^{-10}
Constant: K_2 (mol/l)	7×10^{-5}
Maintenance coefficient on substrate: m_x (per h)	0.014
Maintenance coefficient on oxygen: m_o (per h)	0.467
Constant relating CO_2 to growth: a_1 (mmol CO_2 /g biomass h)	0.143
Constant relating CO_2 to maintenance energy: a_2 (mmol CO_2 /g biomass h)	4×10^{-7}
Constant relating CO_2 to penicillin production a_3 (mmol CO_2 /l h)	10^{-4}
Maximum specific growth rate: μ_x (per h)	0.092
Contois saturation constant: K_x (g/l)	0.15
Oxygen limitation constant: K_{ox}, K_{op} (no limitation)	0
Oxygen limitation constant: K_{ox}, K_{op} (with limitation)	2×10^{-2}
Specific rate of penicillin production: μ_p (per h)	$.5 \times 10^{-4}$
Inhibition constant: K_p (g/l)	0.005
Inhibition constant for product formation: K_I (g/l)	0.0002
Constant: p	0.10
Penicillin hydrolysis rate constant: K (per h)	3
Arrhenius constant for growth: k_g	0.04
Activation energy for growth: E_g (cal/mol)	7×10^3
Arrhenius constant for cell death: k_d	5100
Activation energy for cell death: E_d (cal/mol)	10^{33}
Density x heat capacity of medium: ρC_p (per 1 °C)	50,000
Density heat capacity of cooling liquid: $r_c C_{pc}$ (per 1 °C)	1/1500
Yield of heat generation: r_q (cal/g biomass)	1/2000
Constant in heat generation: r_{q2} (cal/g biomass h)	60
Heat transfer coefficient of cooling/heating liquid: a (cal/h °C)	1.6783×10^{-4}
Cooling water flow rate: F_c (l/h)	1000
Constant: b	0.60
Constants in K_{la} : α, β	70, 0.4
Constant in F_{loss} : λ (per h)	2.5×10^{-4}
Proportionality constant: γ (mol $[H^+]$ /g biomass)	10^{-5}
<i>Controller parameters (PID)</i>	
pH: (base) K_c, t_I : (h), t_d : (h)	$8 \times 10^{-4}, 4.2, 0.2625$
pH: (acid) K_c, t_I : (h), t_d : (h)	$1 \times 10^{-4}, 8.4, 0.125$
Temperature: (cooling) K_c, t_I : (h), t_d : (h)	70, 0.5, 1.6
Temperature: (heating) K_c, t_I : (h), t_d : (h)	5, 0.8, 0.05

$$\frac{dP}{dt} = \mu_{pp}X - KP - \frac{P}{V} \frac{dV}{dt} \quad (5)$$

in which μ_{pp} is the specific penicillin production rate:

$$\mu_{pp} = \mu_p \frac{S}{(K_p + S + S^2/K_1)} \frac{C_L^p}{(K_{op}X + C_L^p)} \quad (6)$$

The utilization of substrate is assumed to be caused by biomass growth and product formation with constant yields and maintenance requirements of the microorganism as suggested by Bajpai and Reuss in [28] and mentioned in [29].

Glucose:

$$\frac{dS}{dt} = -\frac{\mu}{Y_{x/s}}X - \frac{\mu_{pp}}{Y_{p/s}}X - m_xX + \frac{F_{s_f}}{V} - \frac{S}{V} \frac{dV}{dt} \quad (7)$$

Dissolved O_2 :

$$\frac{dC_L}{dt} = -\frac{\mu}{Y_{x/o}}X - \frac{\mu_{pp}}{Y_{p/o}}X - m_oX + K_{la}(C_L^* - C_L) - \frac{C_L}{V} \frac{dV}{dt} \quad (8)$$

in which K_{la} is a function of agitation power input P_w and flow rate of oxygen f_g as introduced in [35].

$$K_{la} = \alpha \sqrt{f_g} \left(\frac{P_w}{V} \right)^\beta \quad (9)$$

The values of α, β are assigned so that the dependence of penicillin concentration on K_{la} showed a very similar behavior to the predictions of [28].

The fed-batch process operation causes a volume change in the fermentor too. This is calculated by:

$$\frac{dV}{dt} = F + F_{a/b} - F_{loss} \quad (10)$$

in which to consider the effect of acid/base addition on the total volume change of the culture broth, the second term, $F_{a/b}$ has been included [29]. Moreover, F_{loss} has been taken to be a function of temperature and culture volume V of the fermentation broth [29]:

$$F_{loss} = V\lambda(e^{5((T-T_o)/T_v-T_o)} - 1) \quad (11)$$

where T_o and T_v are the freezing and boiling temperatures of the culture medium that were assumed to have the same properties as water, respectively.

The volumetric heat production rate is given as:

$$\frac{dQ_{rxn}}{dt} = r_{q1} \frac{dX}{dt} V + r_{q2} XV \quad (12)$$

where r_{q1} is assumed to be constant and might be treated as a yield coefficient [36].

During the product synthesis phase, when the rate of biomass formation becomes very small there is still significant heat generation from metabolic maintenance activities. Hence, the second term in Eq. (12) is included to account for the heat production during maintenance.

Because the heat generation and CO_2 evolution show similar profiles, their production rate due to growth (dX/dt) and biomass (X) should have the same ratio as a first approximation. Based on this observation, r_{q2} is calculated and tabulated in Table 2 [29].

The energy balance is written based on a coiled type heat exchanger which is suitable for a laboratory scale fermentor [37]:

$$\frac{dT}{dt} = \frac{F}{s_f} (T_f - T) + \frac{1}{V\rho C_p} \times \left[Q_{rxn} - \frac{aF_c^{b+1}}{F_c + (aF_c^b/2\rho_c C_{pc})} \right] \quad (13)$$

The variable CO_2 , from which biomass may be predicted with high accuracy. CO_2 evolution is assumed to be due to growth, penicillin biosynthesis and maintenance requirements [29] as suggested by [38]. The CO_2 evolution is:

$$\frac{d\text{CO}_2}{dt} = \alpha_1 \frac{dX}{dt} + \alpha_2 X + \alpha_3 \quad (14)$$

Here, the values of $\alpha_1, \alpha_2, \alpha_3$ are chosen to give CO_2 profiles similar to the predictions of [38]. CO_2 evolution is nearly the same as oxygen demand for penicillin production using glucose as a substrate and CO_2 evolution trend levels off after the fed-batch switch as expected.

The extended model developed in [29] and mentioned here briefly consists of some differential equations that are solved simultaneously.

3. Predictive controller design

Predictive control has been accepted as a useful advanced industrial control technique in recent years [39]. It took more than 15 years after MPC appeared in industry as an effective means to cope with constraints on the state or the control signal control problems, its mathematical background appeared in a steady framework. The issues of feasibility of the online optimization, stability and performance are acceptably understood for systems described by linear models. Many challenges have been made on these issues for nonlinear systems too, but there are many questions remaining about the practical applications.

MPC is mostly formulated in the state space. The nonlinear system to be controlled is described by a discrete time model [9].

$$x(k+1) = f(x(k), u(k), d(k)), \quad x(0) = x_0 \quad (15)$$

where $x(k)$, $u(k)$, and $d(k)$ denote the state, control, and disturbance respectively. A receding horizon implementation is typically formulated by introducing the following optimization problem.

$$\min \sum_{i=1}^{N_p} x^T(i) Q x(i) + \sum_{i=1}^{N_c} u^T(i) R u(i) \quad \text{s.t.} \quad Ex + Fu \leq \Psi \quad (16)$$

where N_p is the prediction horizon, N_c is the control horizon, and E, F, Ψ are matrices with appropriate dimensions to x and u , which describe the constraints. MPC is performed by determining the control signal using this cost function minimization in each step. But, only the first element of the calculated sequence is applied to the plant and this process is to be continued in next steps for shifted horizons. This optimization problem solves for a sequence of future input changes designed to minimize the objective over a prediction horizon of length N_p [10]. In this setup, yet no disturbance $d(k)$ is supposed to occur.

The weighting matrices, Q , and R are used to trade off setpoint tracking and manipulated variable movement, respectively. Moreover, there are physical constraints on acid and base flow rates and they could not exceed 0.1 ml/h [29] to keep the cells from starving and to avoid all of them being washed out of the bioreactor, but any realistic cool water flow rate is available.

To avoid high computational cost dealing with nonlinear optimization, a linearized model of penicillin fermentation process has been chosen near its working point [40]. In fact, the original model parameters are varying with respect to time but most of them have a small variation range during the entire simulation time. For the variables with wide ranges of variation, such as biomass concentration, the mean of their maximum and minimum value was taken into account as empirically achieved to lead to better performance. Actually, this model would not lead to acceptable performance if process variables vary far from its working point, since some information of the process original model has not been considered. This model consists of six transfer functions [40], since it has three inputs (cool water, acid and base flow rates) and two outputs (temperature and pH). Here the problem mainly is concerned with the transfer function from cool water flow rate to temperature:

$$G_{23} = \frac{B(z)}{A(z)} = \frac{.9234 \cdot 4000 z + .9234}{z^2 + \frac{.1126e5}{.6686e4} z - \frac{.1126e5}{.1126e5}} \quad (17)$$

which is an unstable transfer function. The predictors to predict N_p further control signals are described as in a generalized predictive controller framework (for linear systems) [41]:

$$u(t) = Ru(t-1) + Sy(t) + Ku_c(t) \quad (18)$$

in which $u_c(t)$ is the setpoint; 298 K, $u(t-1)$ is the previous control input, $y(t)$ is the current output and R, S are calculated using the method introduced in [39] and used in [40].

It should be noted that due to the highly nonlinear and open-loop unstable nature of this bioprocess, the MPC formulation is not able to deal efficiently with setpoint tracking. This is mainly due to failures in the ODE solver and hence to reach better performance, the regulation of the temperature to 298 K has coarsely been chosen as a cost function regarding movements of control signal [40]. This method led to a closed form controller, which is much easier than empirically tuning an auto-tuned PID. It is noticeable that the constraints are applied in a suboptimal fashion, whereby candidate solutions exceeding these bounds are instead replaced by the bounds themselves.

The algorithm was implemented in MATLAB and the optimization was solved on-line, at each time step. The sampling time was 0.05 h, which is acceptable for practical use. Prediction and control horizon both selected as 24 h and the weighting factors used were $Q = 1$, and $R = 0.2$ ($\lambda = 0.2$) as mentioned before. Initial conditions

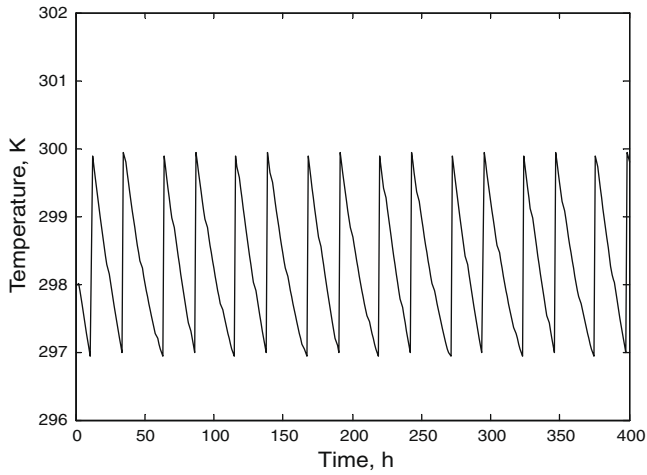


Fig. 2. Temperature with initial substrate and biomass concentrations of 15 g/l and 0.1 g/l, respectively.

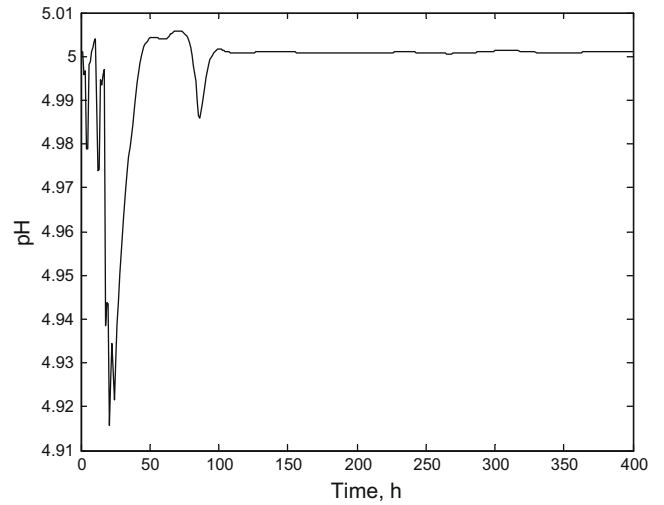


Fig. 4. pH.

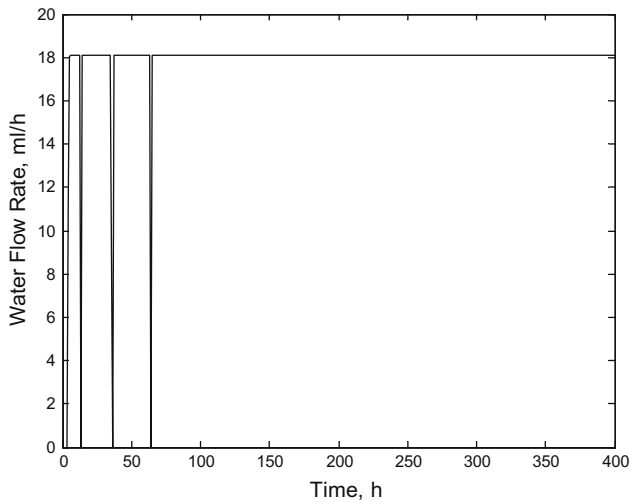


Fig. 3. Cool water flow rate.

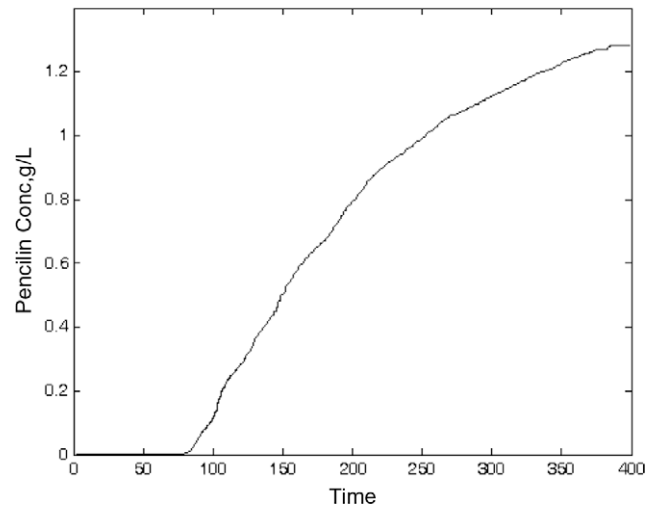


Fig. 5. Penicillin concentration.

are chosen the same as the ones in [29]. The temperature and the control signal, which is cool water flow rate, are shown in Figs. 2 and 3 respectively.

The pH and penicillin concentration are also provided in Figs. 4 and 5 respectively. In this setup, yet pH is to be controlled through a PID controller. As can be seen in the figures, the fluctuations of

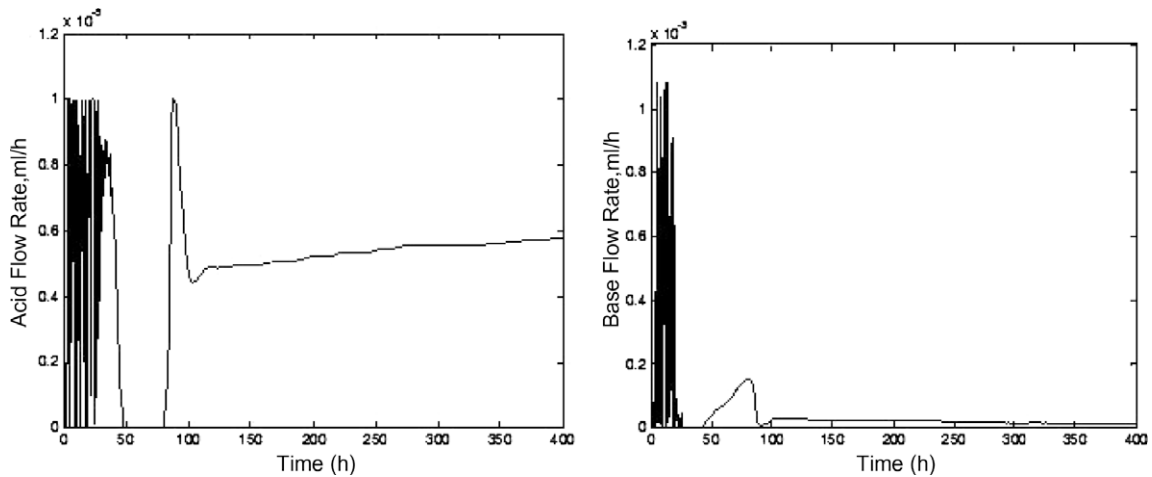


Fig. 6. Acid and base flow rate.

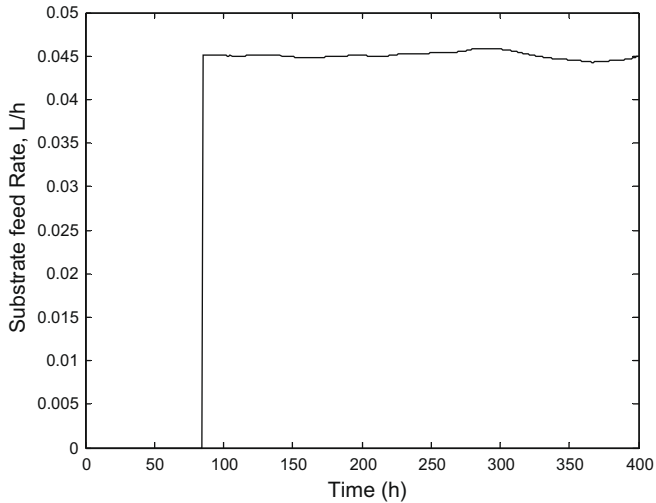


Fig. 7. Substrate feed rate.

the control signals are much less than the ones provided in [29]. The penicillin concentration, which is the final goal, is almost greater than the one mentioned in [29] too, but yet below 1.4 g/l. These are due to using predictive control. Since conventional controllers just make ad-hoc decisions regarding the current error signal, but the predictive controller considers future error signals as well to make a convenient decision. It is noticeable that although temperature has more fluctuations around 298 K, but pH is almost set to 5 without directly being controlled by predictive approach, which is due to their close relationship in the model. The acid, and base flow rates are provided in Fig. 6, and the substrate feed rate is also depicted in Fig. 7. The other parameters can be observed in Fig. 8.

In this part, taking into account the high computational cost of nonlinear optimization, the predictive approach was proposed to control the linearized process. This led to a higher product concentration than the one provided in [29] with less fluctuations of the control signal, which is the cool water flow rate. The merit of this

method is its low computational cost of solving the optimization problem, while leading to a closed form controller, that is much easier than empirically tuning an auto-tuned PID. But, yet better performance could be performed by nonlinear optimization, which is to be discussed in the next section.

4. Nonlinear predictive approach

As mentioned before, due to the highly nonlinear and open-loop unstable nature of this bioprocess, the MPC formulation is not able to deal efficiently with setpoint tracking. This is mainly due to failures in the ODE solver and to the severe ill-conditioning of the optimization problem. To overcome these difficulties and to achieve better performance, the inverse of penicillin concentration has been chosen as a cost function regarding movements of manipulated variables in this section. In addition, the weighting coefficients are chosen such that these two terms have the same order of the magnitude too. Hence, the optimization problem is transformed into the following form:

$$\min 0.001 * \sum_{i=1}^{N_p} 1/P(i) + 10 * \sum_{i=1}^{N_c} \Delta u^T(i) \Delta u(i) \quad \text{s.t.} \quad u_a, u_b \leq 0.1 \quad (19)$$

where the input vector consists of cool water flow rate, acid and base flow rate.

It is noticeable that in this part as well as in Section 3 the optimization problem can be solved for manipulating substrate feed rate as studied in [9,25,42,43] too. However, it is a bit easier to control bioreactors concerning variables, such as pH and temperature, for optimizing the microbial growth [3]. Since these are the ideal variables and often have negligible perturbations. Variables subject to large fluctuations, such as substrate can be a bit difficult to deal with. For instance, too much substrate can be toxic while too little can force an early stationary phase or the onset of endogenous decay (i.e., death by starvation) [9].

As shown in Fig. 9, MPC is performed by determining the control signal by minimizing this cost function in each step regarding the nonlinear original model used for prediction [44,10]. The solu-

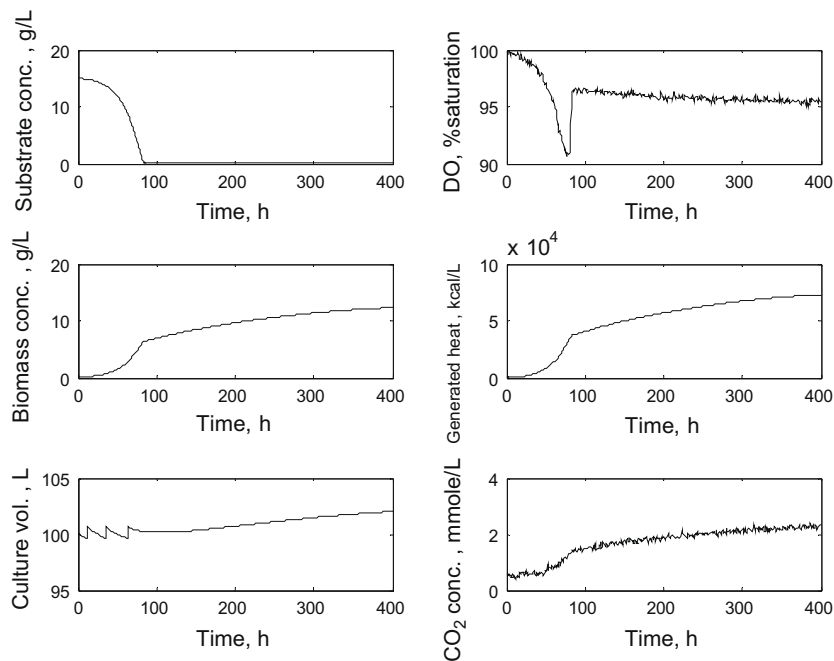


Fig. 8. Other process variables.

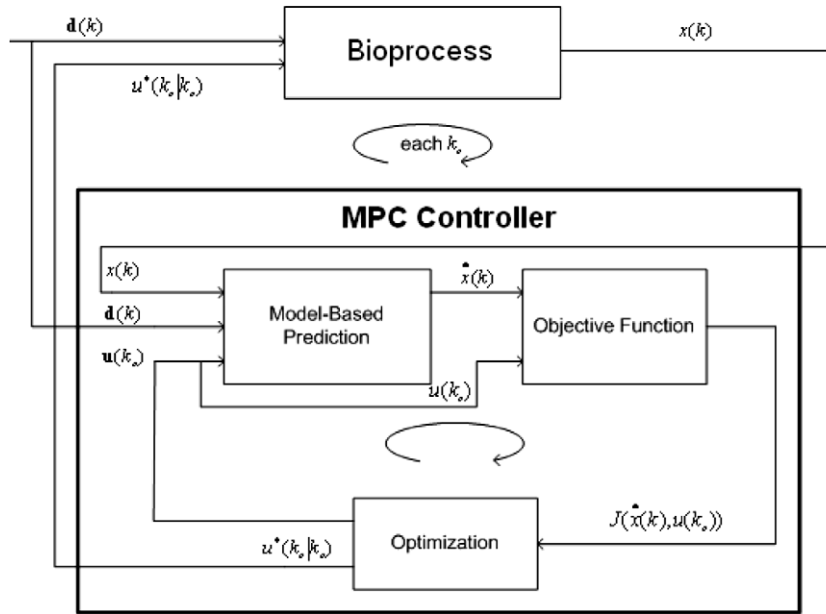


Fig. 9. Bioprocess predictive control block diagram.

tion of this optimization problem is obtained using an SQP-type method. Note that the parameters included in the optimization problem have supposed to be in reach, but if not accessible, they could be estimated by systematic methods using measured data [45].

It is also noticeable that the constraints are not applied in a suboptimal fashion, whereby candidate solutions exceeding these bounds are instead replaced by the bounds themselves (like Section 3). The constraints are considered in the optimization problem instead and this leads to an optimal solution while not moving on the boundary values of constraints.

The algorithm was implemented in MATLAB and the SQP was solved online, at each time step, using the function *fmincon*. The sampling time was 0.05 h, which is acceptable for practical use. Prediction horizon and control horizon are 12 and 9 h respectively and the weighting factors used were $Q = 0.001$, and $R = 10$ as mentioned before. Result for the penicillin concentration trajectory is shown in Fig. 10.

In the controller implementation, input magnitude constraints of $0.0 < u(k) < 0.1$ are imposed for acid and base flow rate. The control signals are provided in Figs. 11 and 12. The substrate feed rate is also depicted in Fig. 13.

As can be seen in the figures, the fluctuations of the control signals are much acceptable than the ones provided in [29], which has large peaks in some small durations. It is also better than the one provided in Section 3. Moreover, the penicillin concentration, which is the final goal, is about 25% greater than the one mentioned in [29] and in Section 3, which is below 1.4 g/l. These are due to using predictive control with that special cost function. Temperature and pH profile are also provided in Figs. 14 and 15 respectively, from which just the temperature varies near the empirical value used in [29], but not the pH. Other process variables are also depicted in Fig. 16. The cost function was also chosen as regulator one to set temperature at 298 K and pH at 5, but the results were not satisfying for the final product concentration.

It must be noted that most of the existing nonlinear model predictive controllers rely on an assumption of the optimization prob-

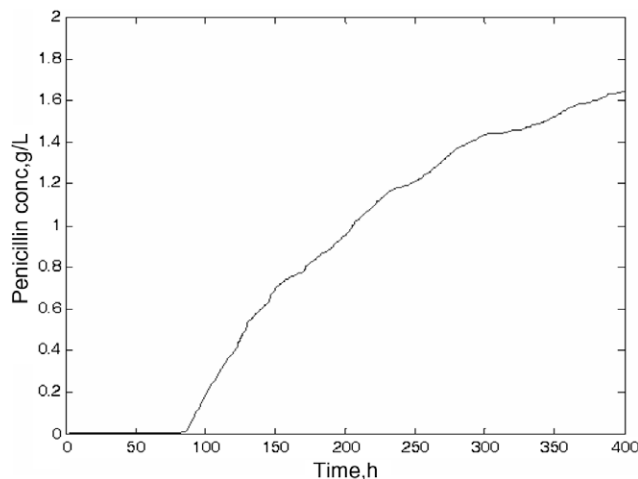


Fig. 10. Penicillin concentration with initial substrate and biomass concentrations of 15 g/l and 0.1 g/l, respectively.

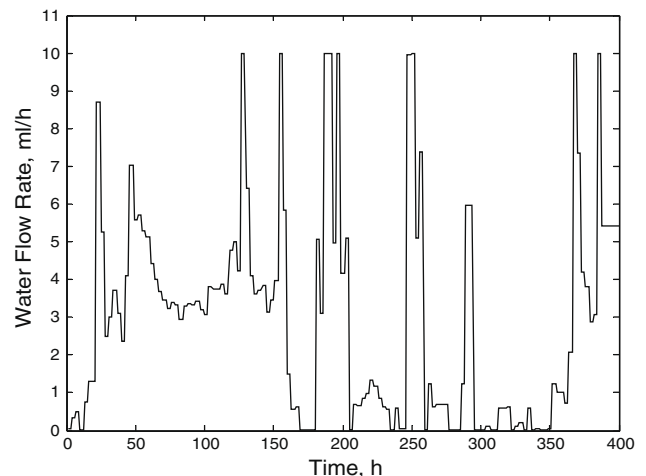


Fig. 11. Cool water flow rate.

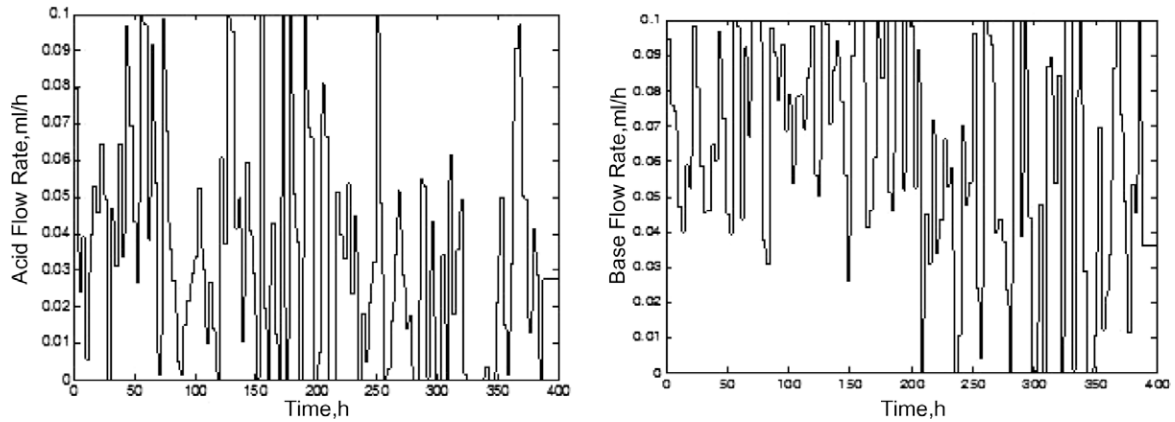


Fig. 12. Acid and base flow rate.

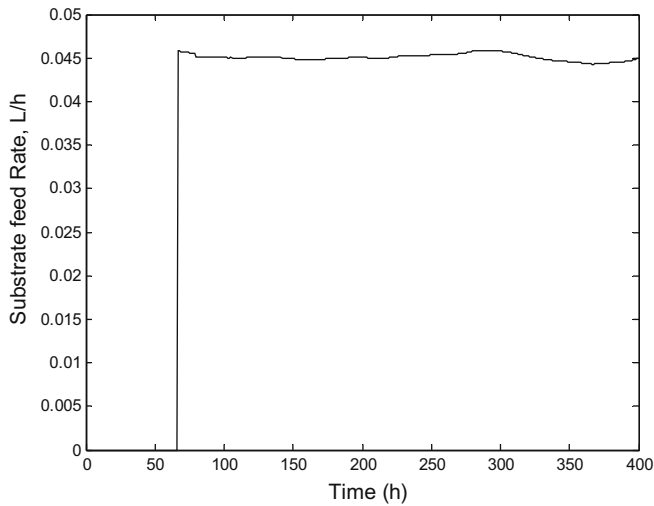


Fig. 13. Substrate feed rate.

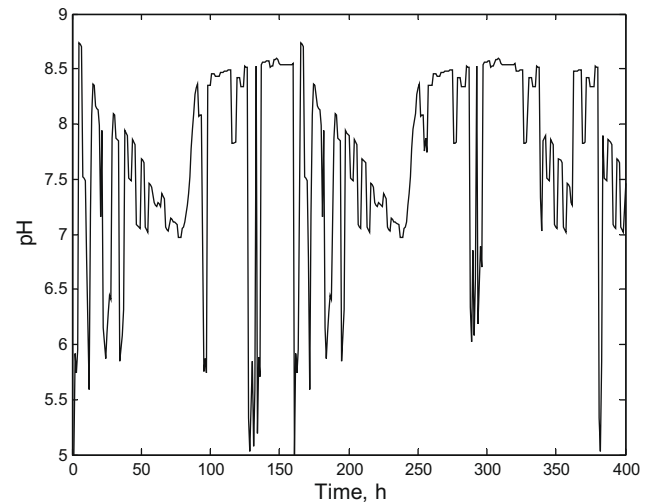


Fig. 15. pH.

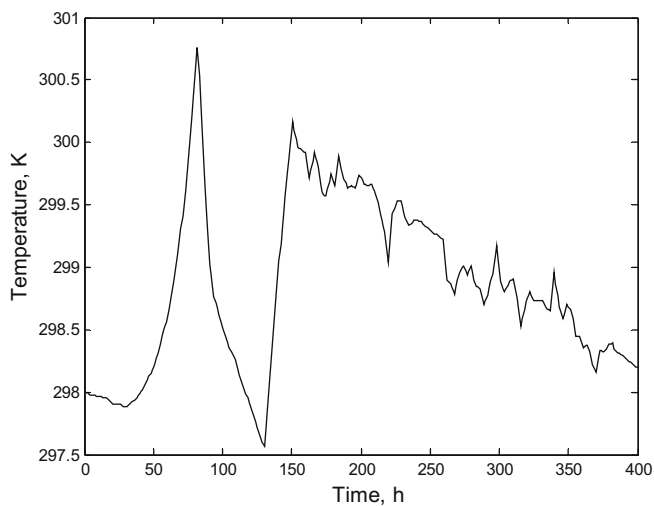


Fig. 14. Temperature.

lem to achieve stabilization. Some recent results on Lyapunov-based model predictive control of nonlinear systems, where appropriate constraints are included in the optimization problem so that

the optimization problem is guaranteed to be feasible have also been achieved. They are based on beginning from a characterized set of conditions, mimicking the stability region obtained by Lyapunov-based bounded controllers, handling input [46] and state constraints [47] as well as uncertainty [48] without resorting to a min-max formulation. The set of mentioned initial conditions could be enhanced as most recently introduced in [49] as well. This paper relies on the aforementioned assumption of achieve stabilization beginning from the same initial condition mentioned in [29]. It can easily be deduced from the figures that the stability has been reached and hence a Lyapunov function exists for this nonlinear predictive framework, which analytically is not easy to find.

5. LoLiMoT based predictive controller

This model defined in Section 2 is definitely nonlinear and hence the optimization problem for predictive controller, which was fully discussed in Section 4, will lead to high computational cost. To overcome this problem, piecewise linear models are utilized to simplify that nonlinear model and finally lessen computational cost. The models are selected using offline identification from the associated data. Moreover, the fuzzy weights of these models are chosen by a neural network, such that the difference between local models output and the nonlinear model output

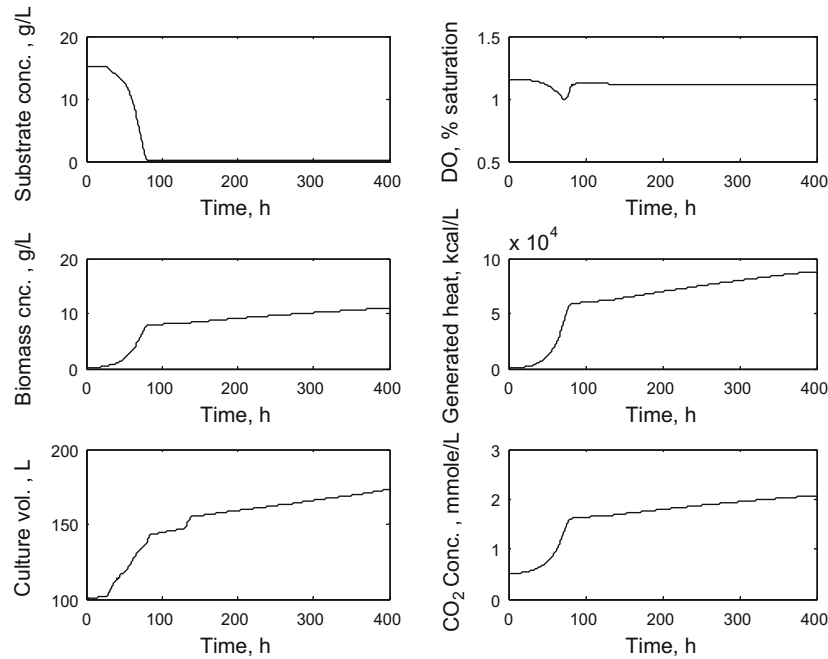


Fig. 16. Other process variables.

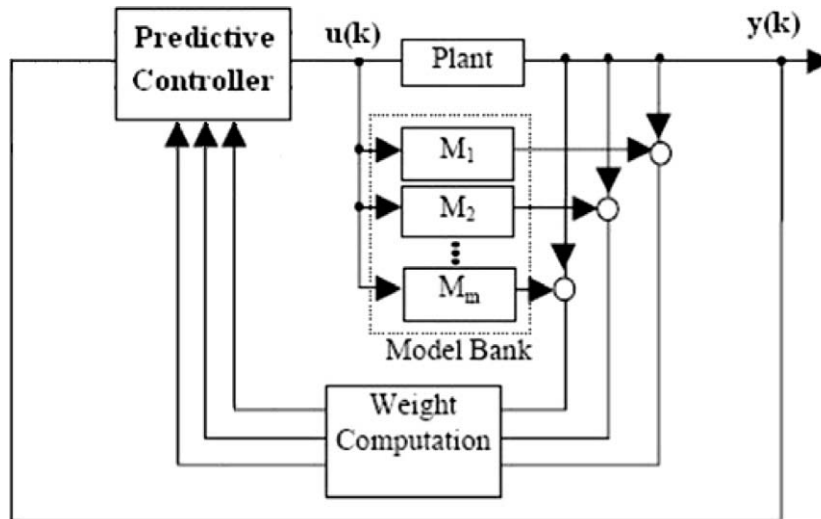


Fig. 17. Multiple-model (including locally linear neuro-fuzzy models) structure.

become as least as possible (Fig. 17). This neural network is trained and used just to build up locally linear neuro-fuzzy (LLNF) models for simplifying the original nonlinear model and the control design remains in predictive framework.

The fundamental approach with the LLNF model is to divide the input space into small linear subspaces with fuzzy validity functions, which describe the validity of each linear model in its region as a fuzzy neuron [50]. Thus, the total model is a neuro-fuzzy network with one hidden layer, and a linear neuron in the output layer, which simply calculates the weighted sum of the outputs of locally linear models (LLMs). These LLMs have basically the same interpretation as Takagi–Sugeno models [23] (with some assumption on parameters), but parameter estimation in TS models is a little bit difficult and hence, that big model is just broken into several smaller LLNF models and LoLiMoT estimates the parameters for these “small” models, which is easier:

$$\hat{y}_i = \omega_{i0} + \omega_{i1}u_1 + \omega_{i2}u_2 + \dots + \omega_{ip}u_p \quad (20)$$

$$\hat{y} = \sum_{i=1}^M \hat{y}_i \phi_i(\underline{u}) \quad (21)$$

where $\underline{u} = [u_1 u_2 \dots u_p]^T$ is the model input, M is the number of LLM neurons, and ω_{ij} denotes the linear estimation parameters of the i th neuron. The validity functions are chosen as normalized Gaussians:

$$\phi_i(\underline{u}) = \frac{\mu_i(\underline{u})}{\sum_{j=1}^M \mu_j(\underline{u})} \quad (22)$$

$$\begin{aligned} \mu_i(\underline{u}) &= \exp\left(-\frac{1}{2}\left(\frac{(u_1 - c_{i1})^2}{\sigma_{i1}^2} + \dots + \frac{(u_p - c_{ip})^2}{\sigma_{ip}^2}\right)\right) \\ &= \exp\left(-\frac{1}{2}\frac{(u_1 - c_{i1})^2}{\sigma_{i1}^2}\right) \times \dots \times \exp\left(-\frac{1}{2}\frac{(u_p - c_{ip})^2}{\sigma_{ip}^2}\right) \end{aligned} \quad (23)$$

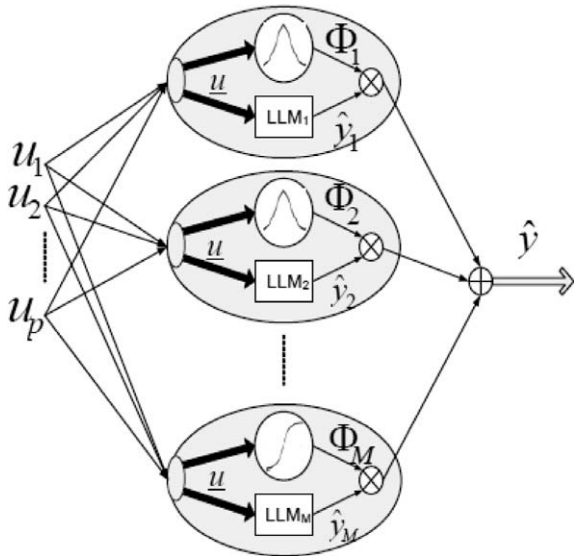


Fig. 18. Topology of locally linear neuro-fuzzy model.

The topology of network is provided in Fig. 18.

The $2M \cdot p$ parameters of the nonlinear hidden layer are the parameters of Gaussian validity functions: center (c_{ij}) and standard deviation (σ_{ij}). Optimization or learning methods are used to adjust the two sets of parameters, the rule consequent parameters of the locally linear models (ω_{ij} 's) and the rule premise parameters of validity functions (c_{ij} 's and σ_{ij} 's). Global optimization of linear consequent parameters is simply obtained by the Least-Squares technique [51,52]. The complete parameter vector contains $M \cdot (p + 1)$ elements:

$$\underline{\omega} = [\omega_{10} \ \omega_{11} \ \dots \ \omega_{1p} \ \omega_{20} \ \omega_{21} \ \dots \ \omega_{M0} \ \dots \ \omega_{Mp}] \quad (24)$$

and the associated regression matrix \underline{X} for N measured data samples is:

$$\underline{X} = [\underline{X}_1 \ \underline{X}_2 \ \dots \ \underline{X}_M] \quad (25)$$

where:

$$\underline{X}_i = \begin{bmatrix} \phi_i(\underline{u}(1)) & u_1(1)\phi_i(\underline{u}(1)) & \dots & u_p(1)\phi_i(\underline{u}(1)) \\ \phi_i(\underline{u}(2)) & u_1(2)\phi_i(\underline{u}(2)) & \dots & u_p(2)\phi_i(\underline{u}(2)) \\ \vdots & \vdots & \ddots & \vdots \\ \phi_i(\underline{u}(N)) & u_1(N)\phi_i(\underline{u}(N)) & \dots & u_p(N)\phi_i(\underline{u}(N)) \end{bmatrix} \quad (26)$$

thus:

$$\hat{y} = \underline{X}\hat{\omega} \quad (27)$$

$$\hat{\omega} = (\underline{X}^T \underline{X} + \alpha I)^{-1} \underline{X}^T y; \quad \alpha \leq 1 \quad (28)$$

α is the regularization parameter for avoiding any near singularity of matrix $\underline{X}^T \underline{X}$ in Eq. (28). The remarkable properties of locally linear neuro-fuzzy model, its transparency and intuitive construction, lead to the use of least squares technique [51,52] for rule antecedent parameters.

An incremental tree-based learning algorithm, e.g. locally linear model tree (LoLiMoT) [50], is appropriate for tuning the rule premise parameters, i.e. determining the validation hypercube for each locally linear model. In each iteration, the worst performing locally linear neuron is determined to be divided. All the possible divisions in the p -dimensional input space are checked and the best is performed. The splitting ratio can be simply adjusted as 0.5; which means that the locally linear neuron is divided into two equal halves. The fuzzy validity functions for the new struc-

ture are updated; their centers are the centers of the new hypercubes, and the standard deviations are usually set as 0.7. The algorithm is as follows:

- (1) *The initial model*: Start with a single locally linear neuron, which is a globally optimal linear least-squares estimation over the whole input space with $\phi_1(u) = 1$ and $M = 1$.
- (2) *Find the worst neuron*: Calculate a local loss function, e.g. MSE for each of the $i = 1, \dots, M$ locally linear neurons, and find the worst performing neuron.
- (3) *Check all divisions*: The worst neuron is considered for further refinement. The validation hypercube of this neuron is divided into two halves with an axis orthogonal split. Divisions in all dimensions are tried, and for each of the p divisions the following steps are carried out:
 - (a) Construction of the multi-dimensional validity functions for both generated hypercubes.
 - (b) Local estimation of the rule consequent parameters for both newly generated neurons.
 - (c) Calculation of the total loss function or error index for the current overall model.
- (4) *Validate the best division*: The best of the p alternatives in Step 3 is selected. If it results in reduction of loss functions or error indices on training and validation data sets, the related validity functions and neurons are updated, the number of neurons is incremented $M = M + 1$; and the algorithm continues from Step 2, otherwise the learning algorithm is terminated.

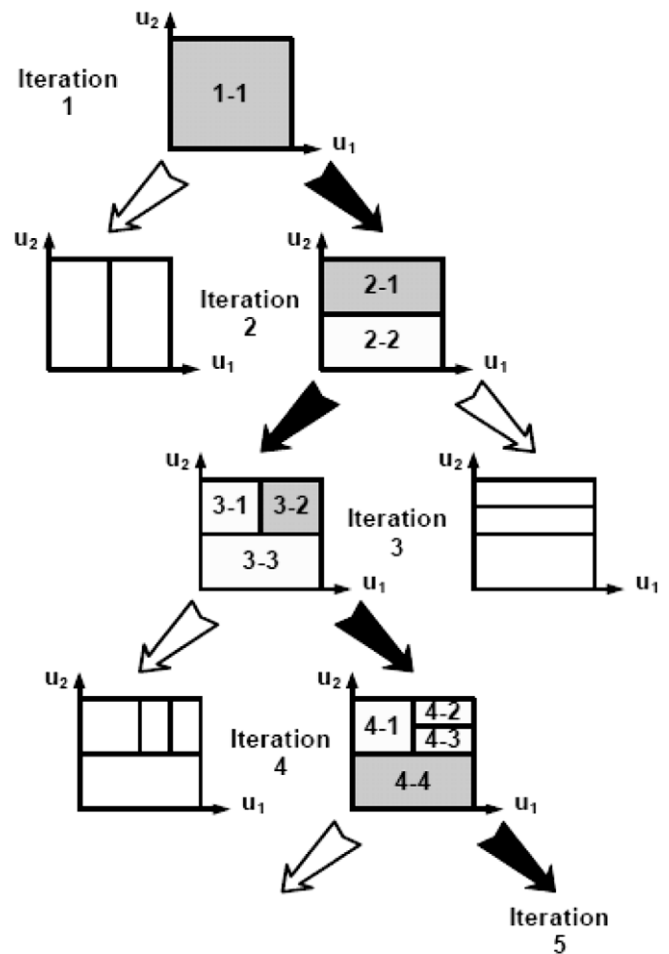


Fig. 19. Five iterations of LoLiMoT algorithm for two-dimensional input space.

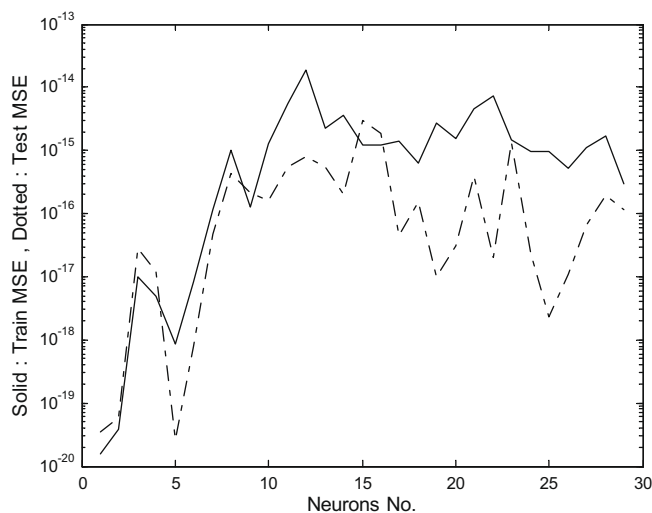


Fig. 20. Training and test error versus the number of the neurons in the middle layer of the neural network used to estimate penicillin concentration.

In Fig. 19, the algorithm is represented for two-dimensional input spaces. This automatic learning algorithm provides the best linear or nonlinear model with maximum generalization, and performs well in prediction applications [53].

As mentioned in the beginning of this section, this algorithm was applied to the nonlinear model output data for each output (so nine networks were trained) in order to get a bank of locally linear models to reduce the optimization computation time for predicting future outputs using this network instead of the original model [53]. If for some outputs the test data error did not form a convex form, in which the minimum is the optimal number of the neurons [50], then it can be deduced that a linear model using a simple method such as LS had sufficed for that output (e.g. Fig. 20 for penicillin concentration output). The final product concentration was as same as the one shown in Fig. 10 and had not changed effectively, but the computational cost as expected reduced almost to one fourth.

6. Conclusion

In this article, taking into account the nonlinearity of the penicillin fermentation process, the predictive approach was proposed to control that. The linear version was applied initially, but acceptable performance was not achieved, hence, the optimization problem was solved to reach the maximum concentration for final product, which is the penicillin while neglecting the empirical setpoints for the temperature and pH. Meanwhile, fluctuations of control signals, which are acid, base and cool water flow rates were also taken into account in order to getting prepared for its practical implementation. This led to a better product than the one provided in [29] with more acceptable fluctuations of control signals. The merit of this method is that it directly solves the optimization problem to obtain maximum possible product concentration, while not violating physical constraints for acid and base flow rates. Moreover, utilizing LoLiMoT based model, the computational cost is also very acceptable for a real time process.

Acknowledgements

The authors want to thank the team working on PENSIM in Illinois Institute of Technology for providing the data for this project.

The authors also want to especially thank Dr. Cinar because of his kind guidance.

References

- [1] J. Liang, Y.Q. Chen, Optimization of a fed-batch fermentation process control competition problem using the NEOS server, *Proceedings of the I MECH E Part I Journal of Systems and Control Engineering* 15 (2003) 427–432.
- [2] A. Johnson, The control of fed-batch fermentation processes: a survey, *Automatica* 23 (6) (1987) 691–705.
- [3] R. Aguilar, J. Gonzalaz, M.A. Barron, R. Martinez-Guerra, R. Maya-Yescas, Robust PI^2 controller for continuous bioreactors, *Process Biochemistry* 36 (2000) 1007–1013.
- [4] J.S. Alford, Bioprocess control: advances and challenges, *Journal of Computers and Chemical Engineering* 30 (2006) 1464–1475.
- [5] F. Renard, A.V. Wouwer, Robust adaptive control of yeast fed-batch cultures, *Journal of Computers and Chemical Engineering* 32 (2008) 1238–1248.
- [6] S. Sugimoto, M. Yabuta, N. Kato, T. Seki, T. Yoshida, H. Taguchi, Hyperproduction of phenylalanine by *Escherichia coli*, *Journal of Biotechnology* 5 (1987) 237–253.
- [7] K.B. Konstantinov, T. Yoshida, A knowledge-based pattern recognition approach for real-time diagnosis and control of fermentation processes as variable structure plants, *IEEE Transactions on Systems, Man, and Cybernetics* 21 (4) (1991) 908–914.
- [8] J. Horiuchi, Fuzzy modeling and control of biological processes, *Journal of Bioscience and Bioengineering* 94 (6) (2002) 574–578.
- [9] S. Ramaswamy, T.J. Cutright, H.K. Qammar, Control of a continuous bioreactor using model predictive control, *Journal of Process Biochemistry* 40 (2005) 2763–2770.
- [10] R.S. Parker, Nonlinear model predictive control of a continuous bioreactor using approximate data-driven models, in: *Proceedings of the American Control Conference*, Anchorage, AK, USA, 2002.
- [11] A.S. Soni, R.S. Parker, Fed-batch bioreactor control using a multi-scale model, in: *Proceedings of the American Control Conference*, Denver, Colorado, USA, 2003.
- [12] B. Dahhou, G. Roux, G. Chamilothoris, Modelling and adaptive predictive control of a continuous fermentation process, *Journal of Applied Math and Modelling* 16 (1992) 545–552.
- [13] R. Schneider, N.A. Jalel, A. Munack, J.R. Leigh, Adaptive predictive control for the fed-batch fermentation process, *Proceedings of the Conference on Control Engineering* 389 (1994) 249–254.
- [14] J.A.D. Rodrigues, R.M. Filho, Production optimization with operating constraints for a fed-batch reactor with DMC predictive control, *Journal of Chemical Engineering Science* 54 (1999) 2745–2751.
- [15] K. Shimizu, An overview on the control system design of bioreactors, *Advances in Biochemical Engineering and Biotechnology* 50 (1993) 65–84.
- [16] K.J. Astrom, Theory and applications of adaptive control: a survey, *Automatica* 19 (5) (1983) 471–486.
- [17] H. Honda, T. Kobayashi, Fuzzy control of bioprocess, *Journal of Bioscience and Bioengineering* 89 (5) (2000) 401–408.
- [18] M. Hosobuchi, F. Fukui, H. Matsukawa, T. Suzuki, H. Yoshikawa, Fuzzy control during microbial production of ML-236B, a precursor of pravastatin sodium, *Journal of Fermentation Technology* 76 (1993) 482–486.
- [19] K.B. Konstantinov, T. Yoshida, An expert approach for control of fermentation processes as variable structure plants, *Journal of Fermentation and Bioengineering* 70 (1990) 48–57.
- [20] K. Oishi, M. Tominaga, A. Kawato, S. Imayasu, S. Nanba, Application of fuzzy control theory to the sake brewing process, *Journal of Fermentation and Bioengineering* 72 (1997) 115–121.
- [21] H. Honda, T. Hanai, A. Katayama, H. Tohyama, T. Kobayashi, Temperature control of Ginjo sake mashing process by automatic fuzzy modeling using fuzzy neural networks, *Journal of Fermentation and Bioengineering* 85 (1998) 107–112.
- [22] C. Karakuzu, M. Turker, S. Ozturk, Modelling, on-line state estimation and fuzzy control of production scale fed-batch baker's yeast fermentation, *Control Engineering Practice* 14 (2006) 959–974.
- [23] T. Takagi, M. Sugeno, Fuzzy identification of systems and its application to modeling and control, *IEEE Transactions on Systems, Man, and Cybernetics* 15 (1) (1985) 116–132.
- [24] Z. Shi, K. Shimizu, Neuro-fuzzy control of bioreactor systems with pattern recognition, *Journal of Fermentation and Bioengineering* 74 (1) (1992) 39–45.
- [25] Hisbullah, M.A. Hussain, K.B. Ramachandran, Design of a fuzzy logic controller for regulating substrate feed to fed-batch fermentation, *Transactions of IChemE* 81 (C) (2003) 138–146.
- [26] C. Valencia, G. Espinosa, J. Giral, F. Giral, Optimization of invertase production in a fed-batch bioreactor using simulation based dynamic programming coupled with a neural classifier, *Computers and Chemical Engineering* 31 (2007) 1131–1140.
- [27] A. Handa-Corrigan, S. Nikolay, D. Fletcher, S. Mistry, A. Young, C. Ferguson, Monoclonal antibody production in hollow fiber bioreactors: process control and validation strategies for manufacturing industry, *Enzyme and Microbial Technology* 17 (3) (1995) 225–230.
- [28] R. Bajpai, M. Reuss, A mechanistic model for penicillin Production, *Journal of Chemical Technology and Biotechnology* 30 (1980) 330–344.

- [29] G. Birol, C. Undey, A. Cinar, A modular simulation package for feed-batch fermentation: penicillin production, *Journal of Computers and Chemical Engineering* 26 (2002) 1553–1565.
- [30] P.R. Patnaik, Penicillin fermentation: mechanisms and models for industrial-scale bioreactors, *Critical Reviews in Microbiology* 27 (1) (2001) 25–39.
- [31] C. Zhao, F. Wang, N. Lu, M. Jia, Stage-based soft-transition multiple PCA modeling and on-line monitoring strategy for batch processes, *Journal of Process Control* 17 (2008) 728–741.
- [32] J. Heijnen, J. Roels, A. Stouthamer, Application of balancing methods in modeling the penicillin fermentation, *Journal of Biotechnology and Bioengineering* 21 (1979) 2175–2201.
- [33] G. Birol, C. Undey, S.J. Parulekar, A. Cinar, A morphologically structured model for penicillin production, *Journal of Biotechnology and Bioengineering* 77 (5) (2002) 538–552.
- [34] M. Schuler, F. Kargi, *Bioprocess Engineering Basic Concepts*, second ed., Prentice Hall, Saddle River, NJ, 2002.
- [35] J.E. Bailey, D.F. Ollis, *Biochemical Engineering Fundamentals*, McGraw Hill, New York, 1986.
- [36] J. Nielsen, J. Villadsen, *Bioreaction Engineering Principles*, Plenum Press, New York, 1994.
- [37] J. Nielsen, *Physiological Engineering Aspects of Penicillin chrysogenum*, World Scientific, Singapore, 1997.
- [38] G. Montague, A. Morris, A. Wright, M. Aynsley, A. Ward, Growth monitoring and control through computer-aided on-line mass balancing in fed-batch penicillin fermentation, *Canadian Journal of Chemical Engineering* 64 (1986) 567–580.
- [39] E.F. Camacho, C. Bordons, *Model Predictive Control*, Springer, 1999.
- [40] A. Ashoori, B. Moshiri, A. Ramezani, M.R. Bakhtiari, A. Khaki-Sedigh, pH control of a fed-batch fermentation process using model predictive control, in: *Proceedings of the 14th International Congress of Cybernetics and Systems of WOSC*, 2008, pp. 730–738.
- [41] D.W. Clarke, C. Mohtadi, P.S. Tuffs, Generalized predictive control. Part I: the basic algorithm, *Automatica* 23 (2) (1987) 137–148.
- [42] M.A. Barro, R. Aguilar, Dynamic behaviour of continuous stirred bioreactor under control input saturation, *Journal of Chemical Technology and Biotechnology* 72 (1998) 15–18.
- [43] R.G. Dondo, D. Marques, Optimal control of a batch bioreactor: a study on the use of an imperfect model, *Process Biochemistry* 37 (2001) 379–385.
- [44] E.S. Meadows, J.B. Rawlings, *Model Predictive Control, Nonlinear Process Control*, Prentice Hall, 1997. pp. 233–310, Chapter 5.
- [45] P. Mhaskar, M.A. Hjortso, M.A. Henson, Cell population modeling and parameter estimation for continuous cultures of *Saccharomyces cerevisiae*, *Biotechnology Progress* 18 (2002) 1010–1026.
- [46] P. Mhaskar, N.H. El-Farra, P.D. Christofides, Predictive control of switched nonlinear systems with scheduled mode transitions, *IEEE Transactions on Automatic Control* 50 (11) (2002) 1670–1680.
- [47] P. Mhaskar, N.H. El-Farra, P.D. Christofides, Stabilization of nonlinear systems with state and control constraints using Lyapunov-based predictive control, *Systems and Control Letters* 55 (2006) 650–659.
- [48] P. Mhaskar, Robust model predictive control design for fault-tolerant of process systems, *Industrial Engineering and Chemical Resources Journal* 45 (2006) 8565–8574.
- [49] M. Mahmood, P. Mhaskar, Enhanced stability regions for nonlinear process systems using model predictive control, *AIChE Journal* 6 (2008) 1487–1498.
- [50] O. Nelles, *Nonlinear System Identification*, Springer-Verlag, Berlin, 2001.
- [51] T. Kariya, H. Kurata, *Generalized Least Squares*, Wiley, 2004.
- [52] J. Wolberg, *Data Analysis Using the Method of Least Squares: Extracting the Most Information from Experiments*, Springer, 2005.
- [53] H. Leung, T. Lo, S. Wang, Prediction of noisy chaotic time series using an optimal radial basis function neural network, *IEEE Transactions on Neural Networks* 12 (2001) 1163–1172.